PHYSICAL REVIEW D **93,** 044055 (2016)

Inequality between size and charge in spherical symmetry

Pablo Anglada, Sergio Dain, and Omar E. Ortiz

Facultad de Matemática, Astronomía y Física, Universidad Nacional de Córdoba, Instituto de Física Enrique Gaviola, IFEG, CONICET, Ciudad Universitaria, 5000 Córdoba, Argentina

(Received 23 December 2015; published 23 February 2016)

We prove that, for a charged spherically symmetric body, twice the radius is always strictly greater than the charge of the body. We also prove that this inequality is sharp. Finally, we discuss the physical implications of this geometrical inequality and present numerical examples that illustrate this theorem.

DOI: 10.1103/PhysRevD.93.044055

I. INTRODUCTION

Consider a body with angular momentum J and electric charge Q. Let $\mathcal{R}$ be a measure of the size of the body. The following inequality is expected to hold for all bodies:

$$\frac{Q^4}{4} + c^2 J^2 \leq k^2 \frac{c^8}{G^2} \mathcal{R}^4, \tag{1}$$

where G is the gravitational constant, c is the speed of light, and k is an universal dimensionless constant. These kinds of inequalities for bodies were presented in [1]. They were motivated by similar kinds of inequalities valid for black holes (see the review article [1] and the references therein). The question of the "minimum size" for a charged object (i.e., the case $J = 0$) was first studied in [2]. Some preliminary results were obtained in [3] for the case $Q = 0$, and in [4] for the case $J = 0$.

Heuristic physical arguments that support the inequality for the case $Q = 0$ were presented in [5] and, in that reference, a version of this inequality was also proved for constant density bodies, using a suitable definition of size. Khuri [6] has proved it in a much more general case, using the same measure of size as in [5]. However, these inequalities are not expected to be sharp.

Recently, Khuri [7] has proved a general version of inequality in the case $J = 0$ using a similar (but not identical) measure of size to the one used in [5] and [6]. As in the previous case, this result is not expected to be sharp.

In these references the inequalities have been studied in the two separated cases $Q = 0$ and $J = 0$. The full inequality (1) was presented for the first time in [8] using a completely different kind of heuristic arguments: they are motivated by the Bekenstein bounds for the entropy of a body. An important property of inequality (1) is that there is only one universal constant k to be fixed. Also, a rigidity statement for inequality (1) was conjectured in [8]: the equality is achieved if and only if the entropy of the body is zero. In general relativity, this statement appears to imply that the equality cannot be achieved for a nontrivial body.

The precise mathematical formulation of inequality (1) involves several difficulties. Perhaps the most severe one is the definition of the size $\mathcal{R}$ for a body in a general spacetime. An appropriate definition of $\mathcal{R}$ is both difficult to find and nonunique. Spherically symmetric spacetimes represent an exception: the area radius of the boundary of the body is a canonical definition of $\mathcal{R}$. The purpose of this work is to study inequality (1) in spherical symmetry (in particular, this implies $J = 0$). We will prove several important properties of inequality (1) which currently cannot be proved in a more general setting. This will also allow us to present the correct setting of the inequality in the general case.

First of all, we determine the universal constant k to be

$$k = 2. \tag{2}$$

Second, we prove that inequality (1) is sharp and strict: the equality cannot be achieved for a nontrivial body. Moreover, the equality is achieved in the asymptotic limit where the radius, charge, and mass of the body tend to zero. This is completely consistent with the argument presented in [8]: the equality implies that the entropy of the body is zero. In particular, a black hole cannot reach the equality in (1) since it always has a nonzero entropy, and hence there is a gap between inequalities for bodies and similar inequalities for black holes (which reach equality for extreme black holes). This gap is given by a difference of a factor of 2 in both inequalities. The existence of this gap is perhaps the most relevant result presented in this article.

Finally, we prove that the correct setting for this inequality is an isolated body that is not contained in a black hole. Inside a black hole, the inequality can be violated. The appropriate definition for a body in this context is, then, a region of asymptotically flat initial data that is not inside a horizon.

The plan of the article is the following. In Sec. II we present our main result given by Theorem 1 and we also discuss in detail its physical implications. In Sec. III we prove Theorem 1. In Sec. IV we present numerical examples that illustrate the assertions in Theorem 1.

Finally, in Appendix we summarize the useful properties of the spherically symmetric initial data set. In the following we use geometrized units where $G = c = 1$.

II. MAIN RESULT

The geometrical inequality between size and charge is appropriately formulated in terms of an *initial data set* for the Einstein equations. For the present results, we restrict ourselves to spherically symmetric initial data where the three-dimensional Riemannian manifold is taken to be $\mathbb{R}^3$. We call them *regular spherically symmetric* initial data. We also assume that the data are *asymptotically flat*. These kinds of data have been extensively studied in a series of articles by Guven and Ó Murchadha [9–11]. In Appendix we summarize their basic properties and definitions.

Let $\partial\mathcal{B}$ be a sphere centered at the origin with area radius $\mathcal{R}$. That is, the area of $\partial\mathcal{B}$ is given by $4\pi\mathcal{R}^2$. The ball enclosed by $\partial\mathcal{B}$ is denoted by $\mathcal{B}$.

For a sphere $\partial\mathcal{B}$ we define the null expansions θ^+ and θ^- by (A32). A region between two concentric balls is said to be *untrapped* if $\theta^+\theta^- > 0$ on that region. The region it is said to be *trapped* if $\theta^+\theta^- < 0$. The outer boundary of a trapped region on asymptotically flat data is called a *horizon* and it satisfies $\theta^+\theta^- = 0$. The area radius of the horizon is denoted by $\mathcal{R}_0$.

Theorem 1.—Consider a regular spherically symmetric, asymptotically flat initial data set. Assume that there exists a ball $\mathcal{B}$ with finite radius $\mathcal{R}$ such that, outside $\mathcal{B}$, the data satisfy the electrovacuum constraint equations. Assume also that in $\mathcal{B}$ the dominant energy condition holds. Let Q be the total charge of $\mathcal{B}$, where we assume $Q \neq 0$. Then,

(i) If the exterior region outside $\mathcal{B}$ is untrapped, the inequality

$$2\mathcal{R} > |Q| \tag{3}$$

holds.

(ii) If there is a horizon outside $\mathcal{B}$, then the radius $\mathcal{R}_0$ of the horizon satisfies the inequality

$$\mathcal{R}_0 \geq |Q|. \tag{4}$$

The equality in (4) is achieved for the horizon of the extreme Reissner-Nordström black hole.

Moreover, we have the following.

(a) Inequality (3) is sharp in the following sense: there exists a sequence of initial data that satisfy the entire hypothesis of item (i) and such that, in the limit, the equality in (3) is achieved. In this limit, the radius, the charge, and the total mass of this sequence tend to zero.

(b) The hypothesis of asymptotic flatness is necessary: there are examples of initial data which are not asymptotically flat but which otherwise satisfy the entire hypothesis in (i) for which inequality (3) is violated.

(c) In case (ii) there are examples where the radius $\mathcal{R}$ of the ball $\mathcal{B}$ (which is inside the horizon) violates the inequality $2\mathcal{R} > |Q|$.

Let us discuss the scope and the physical implications of this theorem. As mentioned in the Introduction, the original motivation to conjecture an inequality of form (3) for bodies comes from the analogous kind of inequalities valid for black holes, namely, in our present setting, inequality (4). In Ref. [12] it has been shown that inequality (4) is valid for general horizons (i.e., no symmetry assumptions), it is a purely quasilocal inequality (i.e., no asymptotically flat assumption is needed) and the equality is achieved for extreme black holes. Since black holes are the "most concentrated objects," one would expect naively that for a fixed charge, the minimum possible radius in an inequality of form (3) is achieved for a black hole. Remarkably, Theorem 1 shows that it is not true: for a fixed charge Q, the minimum possible radius is $|Q|/2$ (and not $|Q|$ as in the case of a black hole). Example (a) shows that this minimum radius is achieved in the asymptotic limit where the radius, the charge, and the total mass of the body (which is not inside a black hole) tend to zero. Nontrivial bodies always satisfy the strict inequality (3). This is consistent with the discussion presented in [8]: the equality in (3) implies that the entropy of the body is zero. Black holes (and also extreme black holes) have nonzero entropy; hence, there should be a gap between inequalities (3) (for bodies) and (4) (for black holes) since the latter saturate for extreme black holes. Theorem 1 shows that this gap is a factor 2.

The canonical definition of a radius in spherical symmetry is the areal radius $\mathcal{R}$. There exists, however, another possible choice for the radius of a ball $\mathcal{B}$: the geodesic distance to the center. However, this radius has the disadvantage that it cannot be used, in general, for a black hole to obtain these kinds of inequalities. The black hole inequalities involve the area of the horizon or quantities that depend, as the area, only on the geometry of the horizon (for example, the shape of the horizon; see [13,14]). The interior of the black hole does not appear to have any physical meaning in this context. In particular, the geodesic distance and also the radius used in [5–7] depend on the interior geometry of the body and hence, in principle, they cannot be applied to black holes. In Theorem 1, for the first time, the same radius definition is used for both bodies and black holes. Finally, we note that for some families of spherically symmetric initial data it can be proved that the geodesic radius is greater than the areal radius (see [10,15]) and hence, for those cases, inequality (3) is also satisfied for the geodesic radius.

As we mentioned above, for a black hole, inequality (4) can be proved without using any asymptotic assumption. It depends only on the local geometry near the horizon. This fact may suggest that a similar result can be proved for a

body $\mathcal{B}$. Namely, making a hypothesis in the interior of the ball $\mathcal{B}$ (regularity and dominant energy condition) and in a neighborhood of the boundary $\partial\mathcal{B}$ (the boundary is untrapped). However, example (b) shows that this is not possible.

Example (c) shows that, inside a black hole, the ball $\mathcal{B}$ with fixed charge Q can be compressed to a radius $\mathcal{R}$ that violates inequality (3). Hence, the hypothesis that the exterior region is untrapped is necessary. Examples (b) and (c) both show that the correct setting for inequality (3) in general (i.e., without any symmetry assumption) is the following: on an asymptotically flat initial data, we consider a region that is not contained in a black hole. This region is the appropriate definition of an "ordinary body" in this context. These are precisely the hypotheses used in the results presented in [6,7]. We also note that these hypotheses are required for the validity of the Bekenstein bounds for the entropy (see [16,17] and the references therein).

In the spirit of the general results obtained in [6,7] about the existence of a black hole due to the concentration of angular momentum and charge, from Theorem 1 we deduce the following corollary.

Corollary 1.—Consider a regular spherically symmetric, asymptotically flat initial data set. Assume that there exists a ball $\mathcal{B}$ with a finite radius $\mathcal{R}$ such that outside $\mathcal{B}$ the data satisfy the electrovacuum constraint equations. Assume also that in $\mathcal{B}$ the dominant energy condition holds. Let Q be the total charge of $\mathcal{B}$. If

$$2\mathcal{R} \leq |Q|, \tag{5}$$

then there are trapped surfaces enclosing $\mathcal{B}$. Example (c) shows that this corollary is not empty. We will see that, in this example, the data are not time symmetric and not maximal.

III. PROOF OF THEOREM 1

The proof is divided naturally into three parts, given by the following sections: III A, III B, and III C. The exterior region of the ball is, by assumption, an asymptotically flat, spherically symmetric solution of the electrovacuum Einstein equations. Hence, by Birkhoff's theorem, this region is described by the Reissner-Nordström metric, which depends only on two parameters: the mass and the charge. This simple characterization of the exterior region is the key simplification introduced by the assumption of spherical symmetry. However, it turns out that we do not need the full strength of Birkhoff's theorem in the proof. We only need to compute the null expansions of the spheres in terms of the mass and the charge. In Sec. III A, for the sake of completeness, we present a proof of this result. In the spirit of Theorem 1, this proof is constructed purely in terms of the constraint equations, in contrast to a standard proof of Birkhoff's theorem where the full Einstein equations are used.

In Sec. III B we prove inequalities (3) and (4). The key ingredient, introduced by Reiris in [14], is the monotonicity of the Hawking energy (equivalent to the Misner-Sharp energy in spherical symmetry) on untrapped regions.

Finally, in Sec. III C we construct the three important examples (a), (b), and (c). These examples are constructed using charged thin shells.

A. The exterior region

Consider the constraint equations (A25) and (A26) in the exterior region of the ball $\mathcal{B}$. The electrovacuum assumption and the spherical symmetry imply $j = 0$, $\mu_M = 0$, and $\rho = 0$. We first solve Maxwell constraint equations (A28) in the exterior region. For the electric field, we obtain

$$E = \frac{Q}{r^2}, \tag{6}$$

where Q is the total charge of the ball given by (A31). For the magnetic field we obtain a similar solution, but since we assume that there are not magnetic charges, the magnetic field vanishes. Then we have

$$\mu = \frac{Q^2}{8\pi r^4}, \tag{7}$$

and hence the constraint equations (A25) and (A26) reduce to

$$K_r(K_r + 2K_l) - \frac{1}{r^2}(r'^2 + 2rr'' - 1) = \frac{Q^2}{r^4}, \tag{8}$$

$$K_r' + \frac{r'}{r}(K_r - K_l) = 0. \tag{9}$$

From Eq. (9) we obtain

$$r'K_l = (K_r r)'. \tag{10}$$

We multiply equation (8) by $r^4 r'$ and use relation (10) to obtain

$$r'r^4K_r{}^2 + r^4 2K_r(K_r r)' - r'^3 r^2 - 2r^3 r' r'' + r' r^2 - r' Q^2 = 0. \tag{11}$$

We rearrange the terms in Eq. (11) to finally get

$$\begin{aligned}&((K_r r)^2 - r'^2)r^2 r' + (r^2 - Q^2)r' \\ &\quad + (((K_r r)^2)' - 2r' r'')r^3 = 0.\end{aligned} \tag{12}$$

Define the function $f(l)$ by

$$f = \frac{r^2}{4}\theta^+\theta^- = r'^2 - (K_r r)^2, \tag{13}$$

where θ^+ and θ^- are the null expansions defined by (A32). Note that the first term in (12) is proportional to f. We calculate f':

$$f' = 2r'r'' - ((K_r r)^2)'. \tag{14}$$

We find that f' is proportional to the last term of (12). Then, using (13) and (14), we write (12) in the following form:

$$-r^2 r' f - r^3 f' + (r^2 - Q^2) r' = 0 \tag{15}$$

We group the first two terms in (15) as a total derivative to finally obtain

$$-r^2 (fr)' + (r^2 - Q^2) r' = 0. \tag{16}$$

Equation (16) can be integrated explicitly. The function f is given by

$$f = 1 - \frac{2C}{r} + \frac{Q^2}{r^2}, \tag{17}$$

where C is a constant.

Up to now, the calculations have been local. If we assume that the exterior region is asymptotically flat, then the constant C that appears in the function f is the total mass (the Arnowitt-Deser-Misner mass) of the initial data. A simple way to obtain this relation is by using the Misner-Sharp energy defined by

$$\mathcal{E} = \frac{r}{2}\left(1 - \frac{r^2}{4}\theta^+\theta^-\right). \tag{18}$$

Using the definition of f, we write $\mathcal{E}$ in the form

$$\mathcal{E} = \frac{r}{2}(1 - f) = C - \frac{Q^2}{2r}. \tag{19}$$

From this expression we calculate the constant C in terms of $\mathcal{E}$ and Q:

$$C = \mathcal{E} + \frac{Q^2}{2r}. \tag{20}$$

A well-known property of the energy $\mathcal{E}$ is that, at infinity, it is equal to the mass M of the initial data (see [18]):

$$M = \lim_{r\to\infty} \mathcal{E}. \tag{21}$$

Then, taking this limit in Eq. (19) we finally obtain $C = M$, and hence the final expression for $\mathcal{E}$ is given by

$$\mathcal{E} = M - \frac{Q^2}{2r}. \tag{22}$$

We have computed the product of the null expansions $\theta^+\theta^-$ in terms of the parameters M and Q:

$$f = \frac{r^2}{4}\theta^+\theta^- = 1 - \frac{2M}{r} + \frac{Q^2}{r^2}. \tag{23}$$

This formula, together with the formula for $\mathcal{E}$ given by (22), is the only property of the exterior region that will be used in the following steps of the proof.

B. The inequality

In this section we will prove inequalities (i) and (ii). We have proved in the previous section that the product of the null expansions [i.e., the function f defined by (23)] is characterized by only two parameters: the mass M and the charge Q. We treat separately the cases where $M \geq |Q|$ and $M < |Q|$.

1. $M \geq |Q|$ case

Assume that the surface of the ball is located at the value l_0 of the geodesic distance to the center, that is, $\mathcal{R} = r(l_0)$. The exterior region is defined by $r(l)$, with $l \geq l_0$.

If $M \geq |Q|$, then f has two real roots (or one double root in the case of equality) at

$$r_+ = M + \sqrt{M^2 - Q^2}, \qquad r_- = M - \sqrt{M^2 - Q^2}. \tag{24}$$

Note that $r_+ \geq r_-$.

For the exterior region, we have two possibilities: either there exists at least one point l_1 (with $l_1 \geq l_0$) such that $r(l_1) = r_+$ or there is no such a point. Consider the first case. Since $f = 0$ at r_+, the exterior region is not untrapped, and hence we are in case (ii) of the theorem. The horizon of the data is located as follows. If there is only one point l_1 such that $r_+ = r(l)$, we take this point. If there are many points that achieve the value r_+, we take the most exterior one; i.e., if $r(l_1) = r(l_2) = r_+$ and $l_1 > l_2$, we take l_1. Let l_1 be such a point. The asymptotic flatness assumption implies that

$$\lim_{l\to\infty} r(l) = \infty. \tag{25}$$

Then $r(l) > r_+$ for $l > l_1$ [if not, this will contradict the assumption that l_1 is the most exterior point with $r(l) = r_+$]. Hence, there are no trapped surfaces in the region $l > l_1$. Then we have shown that $r(l_1)$ is the horizon of the data. The area radius of the horizon is r_+. Hence we have

$$\mathcal{R}_0 = r_+ = M + \sqrt{M^2 - Q^2} \geq |Q|. \tag{26}$$

This proves inequality (4) of Theorem 1. Note that for extreme Reissner-Nordström (i.e., $M = |Q|$), the equality is achieved in (26).

Consider now the second case. If there are no points l_1, with $l_1 \geq l_0$ such that $r(l_1) = r_+$, then by (25) we find that $r(l) > r_+$ for all $l \geq l_0$. The exterior region is untrapped and we are in case (i) of Theorem 1. We have proved that

$$\mathcal{R} = r(l_0) > r_+ \geq |Q|. \tag{27}$$

We emphasize that a stronger version of inequality (3) is satisfied for that case since, in (27), the factor 2 is absent.

Note that in the previous argument we have not mentioned the radius r_-, but we have instead used $r_- \leq r_+$. For example, the ball $\mathcal{B}$ could be in the region $0 < r < r_-$, which is untrapped. However, since $r_- \leq r_+$ and we have condition (25), in that case there will always be a point l_1 in the exterior region such that $r(l_1) = r_+$.

2. $M < |Q|$ case

The case $M < |Q|$ is the most relevant one and it was proved by Reiris [14]. In what follows, we essentially reproduce Reiris's proof. The crucial ingredient is that the Misner-Sharp energy (18) is monotonic on untrapped regions (see [18,19]). If we assume that in the region $l_1 \leq l \leq l_2$ the dominant energy condition is satisfied and $\theta^- > 0$, $\theta^+ > 0$, then

$$\mathcal{E}(l_1) \leq \mathcal{E}(l_2). \tag{28}$$

We first prove the following result, which is interesting in itself.

Lemma 1.—Consider a regular ball $\mathcal{B}$, such that the dominant energy condition is satisfied on $\mathcal{B}$. If on the boundary $\partial\mathcal{B}$ of the ball $\mathcal{B}$ we have $\theta^- > 0$, $\theta^+ > 0$, then the Misner-Sharp energy of the boundary is non-negative,

$$\mathcal{E}(\partial\mathcal{B}) \geq 0. \tag{29}$$

Note that we are not assuming that the ball is embedded in an asymptotically flat data. This is a quasilocal result that depends only on the interior of the ball.

Proof of Lemma 1.—Denote by l_0 the geodesic radius of the ball $\mathcal{B}$, that is, $\mathcal{R} = r(l_0)$. To prove (29), we argue as follows. There are two cases: the interior of $\mathcal{B}$ is either untrapped or not. Consider the first case. Since we hold that $\theta^- > 0, \theta^+ > 0$ on the boundary, if the interior is untrapped (i.e., $\theta^+\theta^- > 0$), we obtain that $\theta^- > 0$, $\theta^+ > 0$ in $\mathcal{B}$. It is well known that in the limit $l \to 0$ the Misner-Sharp energy is non-negative (see, for example, [20], Sec. 6.1.2). Since in the region $\mathcal{B}$ we have $\theta^- > 0, \theta^+ > 0$, we can use (28) with $l_1 = 0$ and $l_2 = l_0$ to obtain

$$0 \leq \mathcal{E}(0) \leq \mathcal{E}(l_0). \tag{30}$$

For the second case, we have, by assumption, that near the boundary $\theta^+\theta^- > 0$. Hence, if the interior region of $\mathcal{B}$ is not untrapped, there should be a radius $r(l_1)$ in the interior of $\mathcal{B}$ such that $\theta^+\theta^- = 0$. From expression (18) we learn that the energy on $r(l_1)$ is non-negative,

$$0 \leq \mathcal{E}(l_1) = \frac{r(l_1)}{2}. \tag{31}$$

In the region $l_1 \leq l \leq l_0$ we have $\theta^- > 0$, $\theta^+ > 0$, and hence we can use (28) to obtain

$$0 \leq \mathcal{E}(l_1) \leq \mathcal{E}(l_0). \tag{32}$$

■

We continue with the proof. Note that since we have assumed $M < |Q|$, the exterior region is untrapped, and hence we are in case (i) of Theorem 1. Moreover, since the data are asymptotically flat for a large r, we find that $\theta^+ > 0$ and $\theta^- > 0$ and hence, since the exterior region is untrapped, we obtain $\theta^+ > 0$ and $\theta^- > 0$ in the whole exterior region. We can explicitly compute the Misner-Sharp energy $\mathcal{E}$ of the boundary of the ball $\mathcal{B}$ using formula (22) and using Lemma 1 we obtain

$$\mathcal{E}(\partial\mathcal{B}) = M - \frac{Q^2}{2\mathcal{R}} \geq 0. \tag{33}$$

That is,

$$\mathcal{R} \geq \frac{Q^2}{2M}. \tag{34}$$

We use $M < |Q|$ to deduce from (34) the desired inequality,

$$2\mathcal{R} \geq Q. \tag{35}$$

Finally, we prove that inequality (35) is strict; that is, no material ball can achieve the equality in (35). We argue by contradiction. Assume there exists a ball $\mathcal{B}$ such that $2\mathcal{R} = |Q|$. By assumption, the exterior region is untrapped, and hence the function f is positive on that region. We have two cases: $M \geq Q$ and $M < |Q|$. For the first case, we have already proved above that the stricter inequality (27) is satisfied, and hence it is not possible to achieve $2\mathcal{R} = |Q|$ for that case. Consider the second case, $M < |Q|$. We compute the energy E at the boundary

$$\mathcal{E}(\partial\mathcal{B}) = M - \frac{Q^2}{2\mathcal{R}} = M - |Q| < 0, \tag{36}$$

where $2\mathcal{R} = |Q|$. Then the energy is negative, and this contradicts Lemma 1.

C. Examples

We construct in this section examples (a), (b), and (c) of the initial data mentioned in Theorem 1. All of the examples and much of the intuition which led to the very formulation of Theorem 1 were extracted from the study of charged thin shells performed by Boulware [21]. In that reference the complete dynamics of charged thin shells in the spacetime is characterized. However, in this section we construct only initial data solving the constraints in a self-contained manner. We make contact with the spacetime picture just to favor the visualization.

We begin with example (a). Consider the following spherically symmetric metric:

$$h = dl^2 + r^2(l)(d\theta^2 + \sin^2\theta d\phi^2), \tag{37}$$

where the radial function $r(l)$ is given by

$$r(l) = \begin{cases} l & \text{for } l \leq \mathcal{R}, \\ r_{RN}(l) & \text{for } l \geq \mathcal{R}, \end{cases} \tag{38}$$

where $\mathcal{R} > 0$ is an arbitrary constant and $r_{RN}(l)$ is the area radius function corresponding to the Reissner-Nordström metric with mass M and charge Q. That is, $r_{RN}(l)$ is the solution of the following differential equation:

$$r'_{RN}(l) = \left(1 - \frac{2M}{r_{RN}} + \frac{Q^2}{r_{RN}^2}\right)^{1/2}. \tag{39}$$

The integration constant in (39) is fixed by the requirement $r_{RN}(\mathcal{R}) = \mathcal{R}$, and hence the function $r(l)$ defined by (38) is continuous.

The initial data set is prescribed with metric (37) and zero second fundamental form. Metric (37) describes a charged thin shell of radius $\mathcal{R}$: the interior $l \leq \mathcal{R}$ is flat and the exterior is given by the Reissner-Nordström metric. The metric depends on three parameters: $(\mathcal{R}, M, Q)$. However, these parameters are not free if we impose the dominant energy condition on the metric. The dominant energy condition for time symmetric data is equivalent to $R \geq 0$, where R is the scalar curvature of the metric. To compute R, we first calculate the first and second derivatives of the function $r(l)$ defined in (38). For the first derivative, we obtain

$$r'(l) = \Theta(l - \mathcal{R})\left(\left(1 - \frac{2M}{r_{RN}} + \frac{Q^2}{r_{RN}^2}\right)^{1/2} - 1\right) + 1, \tag{40}$$

where $\Theta(x)$ is the step function defined by $\Theta(x) = 0$ for $x < 0$ and $\Theta(x) = 1$ for $x > 0$. For the second derivative, we have

$$r''(l) = \delta(l - \mathcal{R})\left(\left(1 - \frac{2M}{r_{RN}} + \frac{Q^2}{r_{RN}^2}\right)^{1/2} - 1\right) + \Theta(l - \mathcal{R})\left(\frac{M}{r_{RN}^2} - \frac{Q^2}{r_{RN}^3}\right), \tag{41}$$

where δ is the Dirac delta function.

Using (40), (41), and expression (A22) for the scalar curvature R of metric (37), we obtain

$$R = 16\pi\sigma\delta(l - \mathcal{R}) + \Theta(l - \mathcal{R})\frac{2Q^2}{r_{RN}^4}, \tag{42}$$

where we have defined

$$\sigma = \frac{1}{4\pi\mathcal{R}}\left(1 - \left(1 - \frac{2M}{\mathcal{R}} + \frac{Q^2}{\mathcal{R}^2}\right)^{1/2}\right). \tag{43}$$

The dominant energy condition $R \geq 0$ implies $\sigma \geq 0$, and this imposes restrictions on the value of the parameters. A convenient way to express this relation is the following. Define the proper mass of the shell by

$$\mathcal{M} = 4\pi\mathcal{R}^2\sigma. \tag{44}$$

Then, from (43) we obtain

$$M = \mathcal{M} + \frac{Q^2 - \mathcal{M}^2}{2\mathcal{R}}. \tag{45}$$

The dominant energy condition is equivalent to $\mathcal{M} \geq 0$.

To make contact with [21], we note that since the data are time symmetric, the proper time derivative of the radius of the shell is zero in the initial data and hence the 4-velocity of the shell (u^μ in Ref. [21]) is orthogonal to the spacelike hypersurface that defines the data. Then, using Eq. (A9) with $t^\mu = u^\mu$, we conclude that the σ defined by (43) is identical to the σ defined by Eq. (10) in [21]. Hence, the proper mass $\mathcal{M}$ defined by (44) is identical to the one defined in [21]. Note that the proper mass $\mathcal{M}$ is conserved along the evolution (see [21]). Relation (45) is the special case of Eq. (16) in [21] where the time derivative of the radius is zero. We emphasize that we have deduced relation (45) using only the dominant energy condition and the constraint equations. Expression (45) was obtained for the first time in [2]. In [22] this expression was generalized in the form of an inequality for spherical distribution of charged matter momentarily at rest.

To construct example (a), we will further impose that $M < |Q|$. The complete spacetime corresponding to these initial data was obtained in [21]. It is a shell that contracts to a minimum radius $\mathcal{R}$ and then reexpands to infinity; see Fig. 1. The exterior region corresponds to the superextreme Reissner-Nordström spacetime.

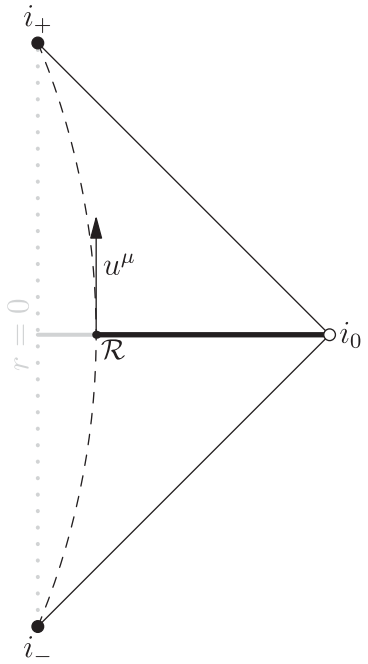

FIG. 1. The dashed line represents the trajectory of the shell. The shell has an infinite radius in the past i_-. It contracts to a minimum radius $\mathcal{R}$ and then reexpands to infinite radius at i_+. The exterior region of the shell corresponds to the superextreme Reissner-Nordström spacetime. The interior region of the shell, drawn in gray, is flat. The spacelike surface of the initial data of example (a) is represented by the thick horizontal line. The velocity of the shell is orthogonal to the initial Cauchy surface.

The sequence of initial data is constructed as follows. We take the following sequence of parameters, where $n \geq 1$ is a natural number:

$$\mathcal{R}_n = \frac{1}{n}, \qquad Q_n = \frac{2}{n} - \frac{1}{n^2}, \qquad \mathcal{M}_n = \frac{1}{2n^3}. \tag{46}$$

This sequence of initial data satisfies the dominant energy conditions since $\mathcal{M}_n > 0$. The total mass is computed using formula (45). We obtain

$$M_n = \frac{1}{n^3} + \frac{2}{n} - \frac{2}{n^2} - \frac{1}{8n^5}. \tag{47}$$

Then we have

$$M_n - Q_n = \frac{8n^2 - 8n^3 - 1}{8n^5} < 0. \tag{48}$$

There are no trapped surfaces in the exterior region, and hence we are in case (i) of Theorem 1. Finally, we also have

$$\frac{Q_n}{2\mathcal{R}_n} = 1 - \frac{1}{2n}. \tag{49}$$

From (49) we find that each member of the sequence satisfies inequality (3), as they should since the data satisfy the hypothesis of the theorem for case (i). Equation (49) implies that the equality in (3) is achieved in the limit $n \to \infty$, and hence we have proved that inequality (3) is sharp. Moreover, in the limit $n \to \infty$, we have

$$\lim_{n\to\infty} Q_n = \lim_{n\to\infty} \mathcal{R}_n = \lim_{n\to\infty} M_n = \lim_{n\to\infty} \mathcal{M}_n = 0. \tag{50}$$

The second example, (b), is constructed using the same metric (37), but with a different choice of parameters. We take $\mathcal{M} > 0$ and

$$|Q| > 2\mathcal{R}. \tag{51}$$

From the definition of $\mathcal{M}$ given by (44) and (43) we deduce that $\mathcal{R} \geq \mathcal{M}$. Using this inequality, formula (45), and assumption (51), we deduce that

$$M > |Q|. \tag{52}$$

In addition, we take $\mathcal{R}$ such that

$$\mathcal{R} < r_-, \tag{53}$$

where r_- is given by (24). We take r_1 such that $\mathcal{R} < r_1 < r_-$ and consider metric (37) defined up to r_1.

These data are, by construction, not asymptotically flat since they have a boundary at r_1. Inequality (3) is not satisfied since we have imposed (51). In the exterior region of $\mathcal{B}$ up to r_1, there are no trapped surfaces. These data are in region III of the Reissner-Nordström spacetime; see Fig. 2.

Finally, we construct the third example, (c). This example is based on the previous example, (b), but the data is extended to reach spacelike infinity. The data are shown in Fig. 3. Note that these data are nontime symmetric. To construct the data, we proceed as follows. Let r_1 and r_2 be two fixed constants that satisfy $\mathcal{R} < r_1 < r_- < r_+ < r_2$. The metric of the data is given by (37), but now the function $r(l)$ is prescribed as follows:

$$r(l) = \begin{cases} l & \text{for } l \leq \mathcal{R}, \\ r_{RN}(l) & \text{for } l \geq \mathcal{R}, \end{cases} \tag{54}$$

where $r_{RN}(l)$ is a solution of the differential equation

$$r'_{RN}(l) = \sqrt{f + (K_r r)^2}, \tag{55}$$

where f is given by (23) and the function K_r is prescribed as follows. The function f is negative in the region $r_- < r < r_+$. Its minimum value,

$$f_{\min} = 1 - \frac{M^2}{Q^2}, \tag{56}$$

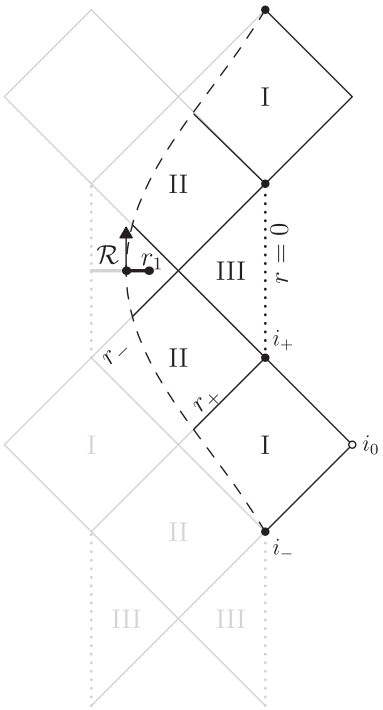

FIG. 2. The initial data of example (b) is a piece of the time symmetric data located in region III of the Reissner-Nordström spacetime.

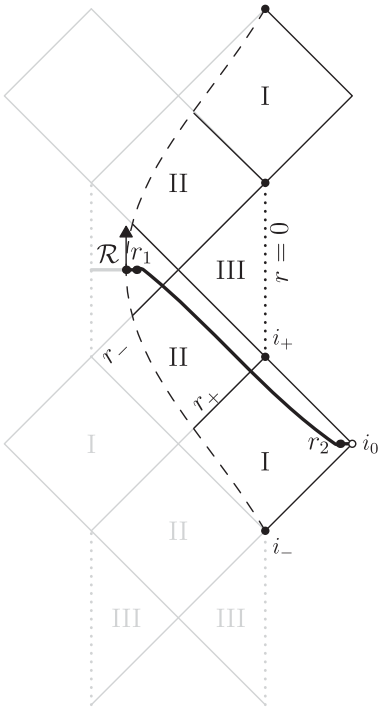

FIG. 3. Example (c) is constructed by extending the surface in example (b) up to spacelike infinity i_0 in region I. The data are time symmetric only in the regions $r < r_1$ and $r_2 < r$.

is achieved at the radius $r_{\min} = Q^2/M$. We prescribe the function $K_r(r)$ to be a smooth function with compact support in $[r_1, r_2]$ such that, on the interval $[r_-, r_+]$, it satisfies

$$(K_r r)^2 > \frac{M^2}{Q^2} - 1. \tag{57}$$

Condition (57) ensures that the radicand on the right-hand side of (55) is always positive, hence

$$r'_{RN} > 0, \tag{58}$$

and we can integrate Eq. (55) to obtain a function $r_{RN}(l)$ which increases monotonically with l. To complete the prescription of the data we calculate the other piece K_l of the second fundamental form using momentum constraint (9), that is,

$$K_l = \frac{r_{RN}}{r'_{RN}} K'_r + K_r. \tag{59}$$

Note that Eq. (59) makes sense only if $r'_{RN} > 0$. We have constructed an asymptotically flat initial data, such that there is a horizon in r_+ and inequality (3) is not satisfied by the ball $\mathcal{B}$. This completes the construction of example (c).

Finally, it is interesting to mention article [23], where the dynamics of two charged thin shells in spherical symmetry is analyzed. This spacetime can provide more sophisticated examples that can have further applications in the study of inequality (3). For the particular choice of parameters made in [23], it is simple to show that inequality (3) is satisfied. In the notation of [23], there are two concentric shells: the exterior one is called shell 2 and the interior one shell 1. There are three regions: the exterior region D_3 outside shell 2, the region D_2 between shell 2 and shell 1, and the interior region inside shell 1 D_1. It is assumed that in D_3 and D_2 the spacetime is superextreme Reissner-Nordström [with parameters (M_3, Q_3) and (M_2, Q_2), respectively], and in D_1 is Minkowski. Clearly, Theorem 1 applies to shell 2 and not to shell 1. Also, since in the exterior region D_3 the spacetime is superextreme Reissner-Nordström, there are no trapped surfaces in D_3, and hence Theorem 1 says that shell 2 should satisfy inequality (3). However, it turns out that, due to the particular assumptions, inequality (3) is also satisfied by shell 1. Let us explicitly prove these two assertions.

The following condition should be satisfied at every shell (see [23]):

$$\mathcal{E}_{A+1} - \mathcal{E}_A > 0, \tag{60}$$

where $A = 1, 2$ and $\mathcal{E}_A$ denote the Misner-Sharp energy in region A. Let us apply (60) to shell 1. Since in D_1 the spacetime is Minkowski, we have $\mathcal{E}_1 = 0$, and hence we obtain

$$\mathcal{E}_2 > 0. \tag{61}$$

Using expression (22) we obtain

$$\mathcal{R}_1 > \frac{Q_2^2}{2M_2}, \tag{62}$$

where $\mathcal{R}_1$ denotes the radius of shell 1. We use the assumption $M_2 < |Q_2|$ on region D_2 to deduce from (62) the desired inequality,

$$\mathcal{R}_1 > \frac{|Q_2|}{2}. \tag{63}$$

Now, we apply (60) to shell 2. We have

$$M_3 - \frac{Q_3^2}{2\mathcal{R}_2} > \mathcal{E}_2, \tag{64}$$

and then

$$\mathcal{R}_2 > \frac{\mathcal{R}_2\mathcal{E}_2}{2M_3} + \frac{Q_3^2}{2M_3}. \tag{65}$$

We use the assumption $M_3 < |Q|_3$ on D_3 and Eq. (61) to finally obtain

$$\mathcal{R}_2 > \frac{|Q_3|}{2}, \tag{66}$$

where $\mathcal{R}_2$ denotes the radius of shell 2.

IV. NUMERICAL EXAMPLES

In Sec. III C we have presented three important examples of initial data that exhibit crucial properties of inequality (3). These examples are constructed in terms of charged thin shells and hence they have distributional curvature. In this section we perform numerical computations of our initial data which have similar properties but are generated by finite smooth matter distribution. These computations are relevant for at least two reasons. First, for each example it will be clear that, by changing slightly the parameters, we obtain a whole family of data that shares the same properties. That is, the examples are generic—they do not depend on a fine-tuning of the parameters. Second, the calculations presented here can have further applications to test similar inequalities with a different definition of radius, like the one presented in [7].

To solve constraint equations (A25) and (A26), we proceed as follows. We use momentum constraint (A26) to calculate K_l as a function of K_r and j, namely,

$$K_l = \frac{r}{r'}K_r' + K_r - 4\pi\frac{r}{r'}j. \tag{67}$$

Note that this equation makes sense only if $r' > 0$. In all our examples with $K_r \neq 0$, this condition is satisfied. Inserting (67) into the Hamiltonian constraint (A25), we obtain

$$3K_r^2 + 2\frac{r}{r'}K_r'K_r - 8\pi\frac{r}{r'}K_r j + \frac{1}{r^2}(r'^2 + 2rr'' - 1) = 8\pi\mu. \tag{68}$$

In Eq. (68) we take the functions $K_r(l)$, $j(l)$, and $\mu(l)$ as free data and we solve for $r(l)$, imposing as initial conditions the regularity conditions for the metric

$$r(0), \qquad r'(0) = 1. \tag{69}$$

It is useful, for testing purposes, to have an integral expression for the energy $\mathcal{E}$. This formula was calculated in [10] and is given by

$$\mathcal{E} = 4\pi\int_0^l dl r^2(\mu r' + jrK_r). \tag{70}$$

In our examples we impose

$$j = 0, \tag{71}$$

and we choose the nonelectromagnetic matter to vanish,

$$\mu_M = 0. \tag{72}$$

Then we have

$$\mu = \frac{1}{8\pi}E^2. \tag{73}$$

The electric field must satisfy the Maxwell constraint equation (A28). We solve this equation as follows: we prescribe a smooth function $Q(l)$ such that, at the origin, $Q(l) = O(l^3)$ and it is constant for $l \geq l_0$, where l_0 represents the geodesic radius of the body.

Then our final equation is given by

$$r'' + \frac{1}{2r}\left((r')^2 - 1\right) = -\frac{Q^2}{2r^3} + \frac{3}{2}r(K_r)^2 + \frac{r^2}{r'}K_rK_r', \qquad r(0) = 0, \quad r'(0) = 1, \tag{74}$$

where both Q and K_r are given functions of l. In [11] it was observed that this initial value problem captures not just solutions representing asymptotically flat initial data. If, for example, the charge is concentrated enough around the origin, then the solution $r(l)$ reaches a maximum and returns to zero at finite geodesic distance. If, on the other hand, r grows big far away from the support regions of K_r and the charge density, then the forcing on the right-hand side vanishes asymptotically and the solution approaches $r' \simeq 1$ and $r'' \simeq 0$, indicating asymptotic flatness. Both of

these behaviors will be shown in the numerical examples below.

A. The implementation

Equation (74) is a simple quasilinear ordinary differential equation (ODE). It can be written as a first order system by defining $u = r$ and $v = r'$,

$$\begin{pmatrix} u \\ v \end{pmatrix}' = \begin{pmatrix} v \\ \frac{1-v^2}{2u} - \frac{1}{2u^3}Q^2(l) + \frac{3}{2}uK_r^2(l) + \frac{u^2}{v}K_r(l)K_r'(l) \end{pmatrix}, \tag{75}$$

with initial condition

$$\begin{pmatrix} u(0) \\ v(0) \end{pmatrix} = \begin{pmatrix} 0 \\ 1 \end{pmatrix}. \tag{76}$$

Now the geodesic distance l can be discretized with a small step size δl and the problem solved with a standard ODE solver. We compute the numerical solutions of (75) and (76) using the standard Runge-Kutta, fourth order accurate method.

We check the pointwise convergence of our code by computing a precision quotient that depends on three numerical solutions to the same problem computed using three different step sizes, δl, $2\delta l$, and $4\delta l$ (see [24]). This quotient should keep close, as a function of l and besides some isolated peaks, to the value 2^4 if the code is correct and the time step is small enough, so that the truncation error is $\mathcal{O}(\delta l^4)$ for the three solutions.

A numerically computed solution will be a fourth order accurate approximation of an exact solution if the latter is at least a C^6 smooth function of l. This is so because the coefficient of the leading term in the truncation error is proportional to the sixth derivative of the exact solution. To obtain a solution C^6 smooth, one needs to prescribe a forcing which is C^4 smooth as a function of l. To this end we introduce a monotonic polynomial, obtained via Hermite interpolation,

$$\begin{aligned} p(a,b,x) &= (1+w)^5(1-5w+15w^2-35w^3+70w^4), \\ w &= \frac{x-b}{b-a}, \\ q(c,d,x) &= 1-p(c,d,x). \end{aligned} \tag{77}$$

For $a \le x \le b$, $p(a,b,x)$ is a monotonically increasing polynomial that matches 0 with 1 in a C^4 smooth way. For $c \le x \le d$, $q(c,d,x)$ is a monotonically decreasing polynomial that matches 1 with 0 in a C^4 smooth way.

Energy integral (70) is approximated by a fourth order accurate composite Simpson's rule. Also, as in the exterior region the energy and the mass satisfy (22), we can compute the mass for any solution computed on a finite l interval that includes a portion of the exterior region.

B. Example (a)

Here we compute the first few members of a sequence $\{r_n(l)\}, n = 2, 3, \ldots$ of regular solutions to problem (74) that saturate inequality (3) in the limit $n \to \infty$. This sequence must have the property that the total charge Q_n vanishes in the limit $n \to \infty$, and, consequently, the areal radius of the charge must also vanish in that limit, so that $\lim_{n\to\infty} 2\mathcal{R}_n/Q_n = 1$.

All solutions in this sequence correspond to time symmetric initial data; that is, in all of these cases we set $K_r = 0$ in the forcing of Eq. (74).

We choose to compute the first few solutions of a sequence that satisfies

$$Q_n = \frac{2}{n} \quad \text{and} \quad \mathcal{R}_n = \frac{1}{n} + \frac{1}{n\ln(n)}, \quad n = 2, 3, 4, \ldots. \tag{78}$$

This sequence of solutions is designed to saturate inequality (3) in the limit $n \to \infty$ as

$$\frac{2\mathcal{R}_n}{Q_n} = 1 + \frac{1}{\ln(n)}, \tag{79}$$

with a slow convergence to one.

Using the polynomial $p(a,b,x)$ defined in (77), we prescribe the function $Q(l)$ to be

$$\begin{aligned} Q(l) &= \begin{cases} Q_n p(a, l_0, l), & \text{if } l < l_o, \\ Q_n, & \text{if } l \ge l_0, \end{cases} \\ a &= 0, \quad l_0 > 0, \quad Q_n = \frac{2}{n}, \end{aligned} \tag{80}$$

where l_0 is the geodesic radius of the charge distribution. At the origin the function $Q(l)$ vanishes as $\mathcal{O}(l^5)$.

To compute each solution of the sequence—say, with index n—the value of the total charge Q_n and the geodesic radius l_0 of the charge are input parameters in the program. The areal radius of the charge $\mathcal{R}(l_0)$ is known only after the solution is computed. Thus, the input parameter l_0 needs to be adjusted to obtain the desired value $\mathcal{R}(l_0) = \mathcal{R}_n$. To adjust l_0, we start with two solutions with the right charge, one with a smaller value of $\mathcal{R}$ and another with a larger value of $\mathcal{R}$. We then perform a bisection procedure on l_0 to find the root of the function

$$g(l_0) = \mathcal{R}(l_0) - \frac{1}{n} - \frac{1}{n\ln(n)}. \tag{81}$$

We stop the iterations when the value of $\mathcal{R}(l_0)$ reaches the value of $\mathcal{R}_n$ with ten correct digits. Table I shows the relevant input parameters we obtain for the first few members of the sequence of solutions and the mass that results for each of them.

TABLE I. Parameters and mass for the first solutions in the sequence satisfying (78).

n	Q_n	δl	l_0	Mass
2	1	1×10^{-3}	1.346158647537232	0.680983
3	2/3	1×10^{-3}	$7.422593683004379 \times 10^{-1}$	0.554538
4	1/2	5×10^{-4}	$5.176483931019902 \times 10^{-1}$	0.449646
5	2/5	5×10^{-4}	$3.981155012268573 \times 10^{-1}$	0.375407
6	1/3	5×10^{-4}	$3.235192440450192 \times 10^{-1}$	0.321540
7	2/7	2×10^{-4}	$2.724420906044543 \times 10^{-1}$	0.280995
8	1/4	1×10^{-4}	$2.352533040568233 \times 10^{-1}$	0.249473

To illustrate the behavior of the solutions in this sequence, two plots are shown. Figure 4 shows the plots of $2r(l)$ and $Q(l)$ of the first ($n = 2$) and last ($n = 8$) solutions in Table I in a small region around the charge domain. Figure 5 shows the plots of $r'(l)$ for all solutions in Table I in a larger region. These last plots show how the solutions satisfy the asymptotic boundary condition. Note that $|r'| \leq 1$: this is always true for time symmetric initial data; see [11].

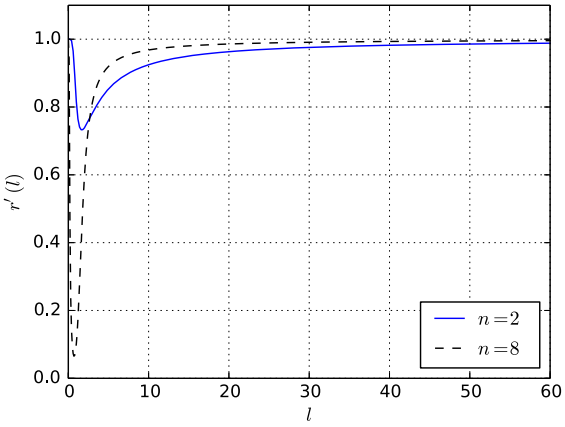

FIG. 5. Plots of $r'(l)$ for the solutions with $n = 2$ and $n = 8$ of Table I (showing asymptotic flatness).

C. Example (b)

In this section we present a single numerical solution representing time symmetric initial data. The charge distribution is a thick spherical shell with support in a finite interval $0 < a \leq l \leq l_0$. The charge $Q(l)$ is given by

$$Q(l) = \begin{cases} 0, & \text{if } l \leq a, \\ Qp(a,b,l), & \text{if } a < l < l_0, \\ Q, & \text{if } l_0 \leq l, \end{cases} \quad a = 0.8, \quad l_0 = 1.0, \quad Q = 2.1. \tag{82}$$

The solution with these parameters violates inequality (3); the total charge Q exceeds $2\mathcal{R}$ by more than 6%. Figure 6 shows a plot of this solution. At about $l = 2.85200$, $r(l)$ gets back to zero. At this point the equation becomes singular and the solution diverges. As expected, $r'(l)$ vanishes outside the body [maximum of $r(l)$] at about $l_1 = 1.72169$, with $r(l_1) = 1.229588$, showing that there exists a trapped surface enclosing the body. However, near the boundary of the body (i.e., in the region $l_0 \leq l < l_1$), there are no trapped surfaces.

As a test for the solution, using formula (22) we calculate the mass $M = 2.408077371$ and then calculate the r_- given by (24). The value of r_- coincides with the value $r(l_1)$ calculated above with seven digits.

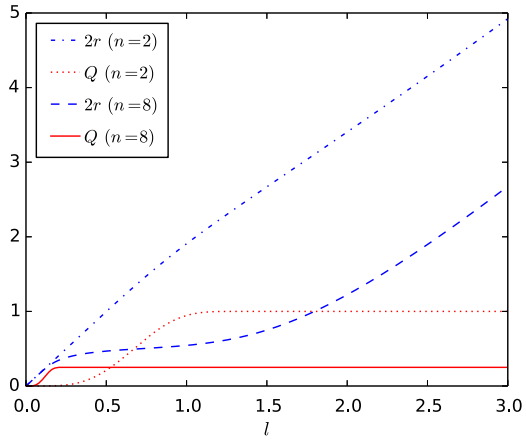

FIG. 4. $2r(l)$ and $Q(l)$ for the solutions with $n = 2$ and $n = 8$. The borders of the objects are placed at the corresponding values of l_0 given in Table I.

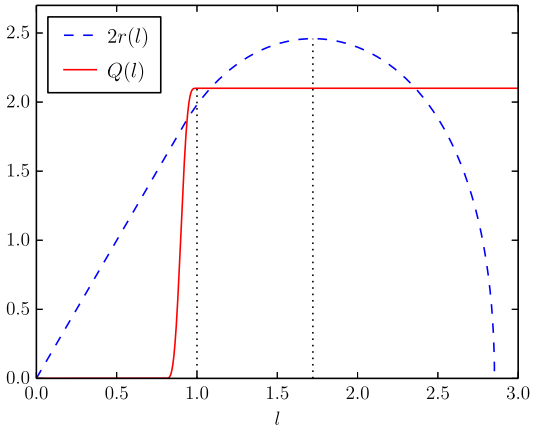

FIG. 6. $2r(l)$ and $Q(l)$ for the solution of example (b), which is not asymptotically flat. The vertical dotted lines indicate the values of $l_0 = 1.0$ (the border of the body) and $l_1 = 1.22959$ where r' becomes zero. Inequality (3) is violated by about 6%.

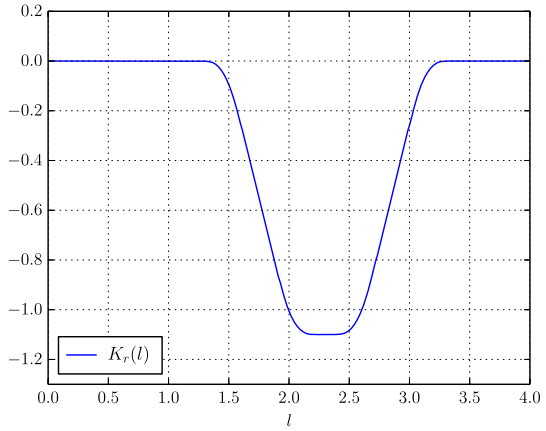

FIG. 7. Plot of $K_r(l)$, C^5 smooth with compact support in [1.2,3.4].

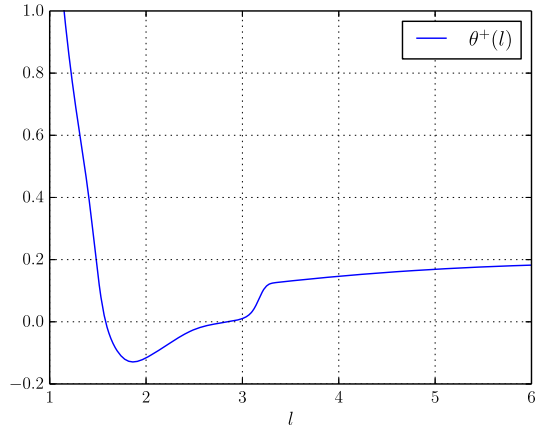

FIG. 9. Plot of $\theta^+(l)$ for the solution of example (c).

D. Example (c)

In this section we modify the data used to obtain the solution of example (b). This is done as suggested by the analytical examples of Sec. III C. The charge distribution is the same as in example (b), so that $Q(l)$ is given by (82), but now there is a nonvanishing extrinsic curvature $K_r(l)$ of compact support. Thus, the solution no longer represents time symmetric initial data. We prescribe $K_r'(l)$ as the C^4 smooth function

$$K_r'(l) = (-2.0) \times \begin{cases} 0, & \text{if } 1.2 \le l, \\ p(1.2, 1.75, l), & \text{if } 1.2 < l \le 1.75, \\ q(1.75, 2.3, l), & \text{if } 1.75 < l \le 2.3, \\ -p(2.3, 2.85, l), & \text{if } 2.3 < l \le 2.85, \\ -q(2.85, 3.4, l), & \text{if } 2.85 < l < 3.4, \\ 0, & \text{if } 3.4 \le l, \end{cases} \tag{83}$$

where p and q are the polynomials defined in (77). $K_r(l)$ is defined as the exact integral of $K_r(l)$. In Fig. 7 we show a plot of K_r.

The solution obtained is a monotonically increasing $r(l)$ coincident with the solution of example (b) when $l \le 1.2$ (the initial value problem is exactly the same up to this point). For larger values of l, the extrinsic curvature affects the solution so that $r(l)$ keeps growing and the solution becomes asymptotically flat. Figure 8 shows the behavior of this solution.

This solution has a horizon outside the body. Figure 9 shows the plot of $\theta^+(l)$. This function has two roots, located at $l^- = 1.58085$ and $l^+ = 2.85231$. These values correspond to radii $r(l^-) = 1.22959$ and $r(l^+) = 3.58657$, respectively. The computed mass for this solution is $M = 2.408077371$. The total charge, $Q = 2.1$, is an input parameter in the program. We can compute the values r_- and r_+ given by Eq. (24), which turn out to be coincident with the values $r(l^-)$ and $r(l^+)$ in seven and six digits, respectively. The radius of the horizon, $\mathcal{R}_0 = r_+$, clearly satisfies inequality (4). Finally, using formula (67) we numerically compute K_l and then compute the trace of the second fundamental form given by $K = K_l + 2K_r$. This function is nonzero, and hence the data are not maximal.

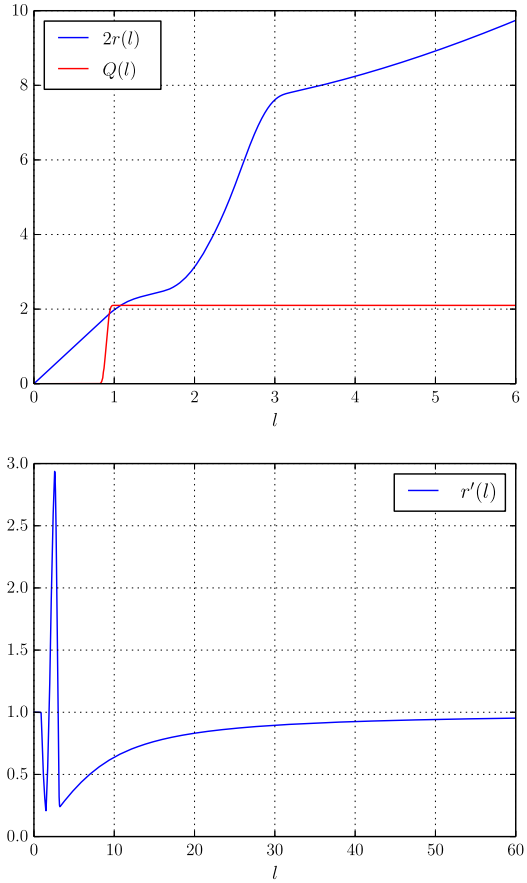

FIG. 8. $2r(l)$ and $Q(l)$ (upper panel), $r'(l)$ on a larger domain (lower panel), for the solution obtained with (82) and (83).

V. FINAL COMMENTS

We have studied the inequality between size and charge for bodies in spherical symmetry. Theorem 1 provides a complete characterization of this inequality. In particular, this result uncovers many important properties of this inequality, like the gap factor 2 between a body and a black hole. The natural question is, how do we generalize this theorem to the nonspherically symmetric case? As we point out in the Introduction, one of the main difficulties in studying this problem is the definition of the size $\mathcal{R}$ for general spacetimes. A naive generalization would be to take the area of the boundary of the body. However, there exist explicit counterexamples to the inequality using this measure of size [25]. Moreover, it is unlikely that a definition of size that takes into account only properties of the boundary will work in the general case. In fact, the size definitions used in [5] and [7] depend on the interior of the body. However, these definitions do not reduce to the area in the spherically symmetric case. Hence, they will not provide sharp results, like the rigidity or the gap factor proved in Theorem 1.

A new definition of size was presented in [8]. It is based on the inverse mean curvature flow. This definition reduces to the area radius in spherical symmetry and also depends on the interior of the body. How to generalize Theorem 1 using this definition of size is a relevant open problem.

ACKNOWLEDGMENTS

This work was supported by Grant No. PIP of CONICET and by Grants No. 05-B454 and No. 05-B545 of Secretaría de Ciencia y Tecnología, Universidad Nacional de Córdoba.

APPENDIX: SPHERICALLY SYMMETRIC INITIAL DATA FOR THE EINSTEIN-MAXWELL EQUATIONS

Let M be a four-dimensional manifold with metric $g_{\mu\nu}$ [with signature $(-+++)$] and Levi-Civita connection ∇_μ. In the following, Greek indices $\mu, \nu \cdots$ are always four dimensional.

Consider Einstein equations with energy momentum tensor $T_{\mu\nu}$,

$$G_{\mu\nu} = 8\pi T_{\mu\nu}, \tag{A1}$$

where $G_{\mu\nu}$ is the Einstein tensor of the metric $g_{\mu\nu}$. The *dominant energy condition* for $T_{\mu\nu}$ is given by

$$T_{\mu\nu} v^\mu w^\nu \geq 0 \tag{A2}$$

for all future-directed causal vectors v^μ and w^ν.

It will be useful to decompose the matter fields $T_{\mu\nu}$ into the electromagnetic part and the nonelectromagnetic part,

$$T_{\mu\nu} = T^{EM}_{\mu\nu} + T^{M}_{\mu\nu}, \tag{A3}$$

where $T^{EM}_{\mu\nu}$ is the electromagnetic energy momentum tensor given by

$$T^{EM}_{\mu\nu} = \frac{1}{4\pi}\left(F_{\mu\lambda}F_{\nu}{}^{\lambda} - \frac{1}{4} g_{\mu\nu} F_{\lambda\gamma} F^{\lambda\gamma}\right), \tag{A4}$$

and $F_{\mu\nu}$ is the (antisymmetric) electromagnetic field tensor that satisfies the Maxwell equations

$$\nabla^\mu F_{\mu\nu} = -4\pi \mathcal{J}_\nu, \tag{A5}$$

$$\nabla_{[\mu} F_{\nu\alpha]} = 0, \tag{A6}$$

where $\mathcal{J}_\nu$ is the electromagnetic current.

Initial conditions for Einstein equations are characterized by the initial data set given by $(\Sigma, h_{ij}, K_{ij}, \mu, j^i)$, where Σ is a connected three-dimensional manifold, h_{ij} a (positive definite) Riemannian metric, K_{ij} a symmetric tensor field, μ a scalar field, and j^i a vector field on Σ, such that the constraint equations

$$D_j K^{ij} - D^i K = -8\pi j^i, \tag{A7}$$

$$R - K_{ij}K^{ij} + K^2 = 16\pi\mu \tag{A8}$$

are satisfied on Σ. Here, D and R are the Levi-Civita connection and the scalar curvature associated with h_{ij}, and $K = K_{ij}h^{ij}$. Latin indices $i, k, \ldots$ are three dimensional, and they are raised and lowered with the metric h_{ij} and its inverse h^{ij}. For a general introduction to this subject, see, for example, review article [26] and the references therein.

If we think of the initial data as a spacelike surface in the spacetime, with unit timelike normal t^μ, then the matter fields μ and j^i are given in terms of the energy momentum tensor $T_{\mu\nu}$ by

$$\mu = T_{\mu\nu} t^\mu t^\nu, \qquad j_\nu = T_{\mu\nu} t^\nu. \tag{A9}$$

The dominant energy condition (A2) implies

$$\mu^2 \geq j_i j^i. \tag{A10}$$

The decomposition (A3) of the matter fields translates to

$$\mu = \mu_{EM} + \mu_M, \qquad j^i = j^i_{EM} + j^i_M, \tag{A11}$$

where we have defined

$$\mu_{EM} = \frac{1}{4\pi}(E^i E_i + B^i B_i), \qquad j^i_{EM} = \epsilon^i{}_{jk} E^j B^k, \tag{A12}$$

where ϵ_{ilm} is the volume element of h_{ij}, and the electric field E and the magnetic field B are given by

$$E_\mu = F_{\mu\nu}t^\nu, \qquad B_\mu = -{}^*F_{\mu\nu}t^\nu, \tag{A13}$$

where ${}^*F_{\mu\nu}$ denotes the dual of $F_{\mu\nu}$ defined with respect to the volume element $\epsilon_{\mu\nu\lambda\gamma}$ of the metric $g_{\mu\nu}$ by the standard formula

$${}^*F_{\mu\nu} = \frac{1}{2}F^{\alpha\beta}\epsilon_{\alpha\beta\mu\nu}. \tag{A14}$$

The electric and magnetic fields satisfy the Maxwell constraint equations

$$D^iE_i = 4\pi\rho, \qquad D^iB_i = 0, \tag{A15}$$

where ρ is the electric charge density. The relation between ρ and the spacetime electromagnetic current $\mathcal{J}^\mu$ is given by $\rho = \mathcal{J}^\mu t_\mu$.

The initial data model an isolated system if the fields are weak far away from sources. This physical idea is captured in the following definition of asymptotically flat initial data set. In this article we assume that the manifold Σ is $\mathbb{R}^3$, and hence the definition simplifies slightly. Consider Cartesian coordinates x^i, with their associated Euclidean radius $r = (\sum_{i=1}^3 (x^i)^2)^{1/2}$, and let δ_{ij} be the Euclidean metric components with respect to x^i. The initial data set $(\Sigma, h_{ij}, K_{ij}, \mu, j^i)$ is called asymptotically flat if the metric h_{ij} and the tensor K_{ij} satisfy the following falloff conditions:

$$h_{ij} = \delta_{ij} + \gamma_{ij}, \qquad K_{ij} = O(r^{-2}), \tag{A16}$$

where $\gamma_{ij} = O(r^{-1})$, $\partial_k\gamma_{ij} = O(r^{-2})$, $\partial_l\partial_k\gamma_{ij} = O(r^{-3})$, and $\partial_k K_{ij} = O(r^{-3})$. These conditions are written in terms of Cartesian coordinates x^i. Here, ∂_i denotes partial derivatives with respect to these coordinates.

We will assume that the initial data set has spherical symmetry. The ξ^i is one of the Killing vectors that generates the group $SO(3)$, so we say that the initial data set is *spherically symmetric* if

$$\mathcal{L}_\xi h_{ij} = \mathcal{L}_\xi K_{ij} = \mathcal{L}_\xi \mu = \mathcal{L}_\xi j^i = 0, \tag{A17}$$

for all generators ξ of $SO(3)$, where $\mathcal{L}$ denotes the Lie derivative. Note that we are also imposing spherical symmetry on the sources. We also impose this condition on the electromagnetic field:

$$\mathcal{L}_\xi E^i = \mathcal{L}_\xi B^i = \mathcal{L}_\xi \rho = \mathcal{L}_\xi j^i_{EM} = 0. \tag{A18}$$

There are several useful coordinates to describe spherically symmetric metrics. In this article we will use the geodesic coordinates given by

$$h = dl^2 + r^2(l)(d\theta^2 + \sin^2\theta d\phi^2), \tag{A19}$$

where l is the proper radial distance to the center and $r(l)$ is the areal radius. The function $r(l)$ is assumed to be smooth for $0 \le l < \infty$. Regularity at the center implies the following conditions for $r(l)$:

$$r(0) = 0, \qquad r'(0) = 1, \tag{A20}$$

where the prime denotes the derivative with respect to l. Asymptotically flat condition (A16) implies that

$$\lim_{l\to\infty} r' = 1. \tag{A21}$$

The scalar curvature of metric (A19) is given by

$$R = -\frac{2}{r^2}(r'^2 + 2rr'' - 1). \tag{A22}$$

Let n^i denote the outwards unit normal vector to the spheres centered at the origin; that is, $n = \partial/\partial l$. The general form of the extrinsic curvature in spherical symmetric is given by

$$K_{ij} = n_i n_j K_l + (g_{ij} - n_i n_j)K_r, \tag{A23}$$

where K_l and K_r are two functions of l. Asymptotically flat condition (A16) implies that

$$\lim_{l\to\infty} rK_r = 0. \tag{A24}$$

Using (A22) and (A23), we can write the constraint equations (A7) and (A8) in spherical symmetry in the following form:

$$K_r(K_r + 2K_l) - \frac{1}{r^2}(r'^2 + 2rr'' - 1) = 8\pi\mu, \tag{A25}$$

$$K_r' + \frac{r'}{r}(K_r - K_l) = 4\pi j, \tag{A26}$$

where j is the radial component of the current density $j = j^i n_i$, which is the only nontrivial component due to the spherical symmetry. The dominant energy condition is given by

$$\mu \ge |j|. \tag{A27}$$

Let $E = E^i n_i$ and $B = B^i n_i$. Then, Eq. (A15) is given by

$$\frac{1}{r^2}(Er^2)' = 4\pi\rho, \qquad \frac{1}{r^2}(Br^2)' = 0, \tag{A28}$$

where ρ is the electric charge density. The energy density μ is given by

$$\mu = \mu_M + \frac{1}{8\pi}(E^2 + B^2). \tag{A29}$$

Note that since B^i and E^i are radial, $j^i_{EM} = 0$ and hence the current density j^i has no electromagnetic contribution in spherical symmetry. We say that the data is in *electrovacuum* if $\mu_M = 0$ and $j = 0$.

The electric charge contained in $\mathcal{B}$ is given by

$$Q = 4\pi \int_0^{l_0} \rho r^2 dl. \tag{A30}$$

Using the Gauss theorem and Eq. (A28), we obtain that the charge can also be written as

$$Q = Er^2. \tag{A31}$$

Finally, the outgoing future and past null expansions are given by

$$\theta^+ = \frac{2}{r}(r' + K_r r), \qquad \theta^- = \frac{2}{r}(r' - K_r r). \tag{A32}$$

[1] S. Dain, Geometric inequalities for black holes, Gen. Relativ. Gravit. **46**, 1715 (2014).
[2] R. Arnowitt, S. Deser, and C. Misner, Minimum size of dense source distributions in general relativity, Ann. Phys. (N.Y.) **33**, 88 (1965).
[3] P. R. Anglada, master's thesis, Universidad Nacional de Córdoba, 2013.
[4] M. Rubio, master's thesis, Universidad Nacional de Córdoba, 2014.
[5] S. Dain, Inequality between Size and Angular Momentum for Bodies, Phys. Rev. Lett. **112**, 041101 (2014).
[6] M. A. Khuri, Existence of black holes due to concentration of angular momentum, J. High Energy Phys. 06 (2015) 188.
[7] M. A. Khuri, Inequalities between size and charge for bodies and the existence of black holes due to concentration of charge, J. Math. Phys. (N.Y.) **56**, 112503 (2015).
[8] S. Dain, Bekenstein bounds and inequalities between size, charge, angular momentum and energy for bodies, Phys. Rev. D **92**, 044033 (2015).
[9] J. Guven and N. O. Murchadha, Geometric bounds in spherically symmetric general relativity, Phys. Rev. D **56**, 7650 (1997).
[10] J. Guven and N. O'Murchadha, The constraints in spherically symmetric classical general relativity. I. Optical scalars, foliations, bounds on the configuration space variables and the positivity of the quasilocal mass, Phys. Rev. D **52**, 758 (1995).
[11] J. Guven and N. O'Murchadha, The constraints in spherically symmetric classical general relativity. II. Identifying the configuration space: A moment of time symmetry, Phys. Rev. D **52**, 776 (1995).
[12] S. Dain, J. L. Jaramillo, and M. Reiris, Area-charge inequality for black holes, Classical Quantum Gravity **29**, 035013 (2012).
[13] M. E. Gabach Clément and M. Reiris, Shape of rotating black holes, Phys. Rev. D **88**, 044031 (2013).
[14] M. Reiris, On the shape of bodies in general relativistic regimes, Gen. Relativ. Gravit. **46**, 1777 (2014).
[15] P. Bizon, E. Malec, and N. O'Murchadha, Trapped surfaces due to concentration of matter in spherically symmetric geometries, Classical Quantum Gravity **6**, 961 (1989).
[16] J. D. Bekenstein, How does the entropy/information bound work?, Found. Phys. **35**, 1805 (2005).
[17] R. Bousso, The holographic principle, Rev. Mod. Phys. **74**, 825 (2002).
[18] S. A. Hayward, Gravitational energy in spherical symmetry, Phys. Rev. D **53**, 1938 (1996).
[19] M. A. Khuri, Hoop conjecture in spherically symmetric spacetimes, Phys. Rev. D **80**, 124025 (2009).
[20] L. B. Szabados, Quasi-local energy-momentum and angular momentum in GR: A review article, Living Rev. Relativity **7**, 4 (2004).
[21] D. G. Boulware, Naked singularities, thin shells, and the Reissner-Nordström metric, Phys. Rev. D **8**, 2363 (1973).
[22] P. Koc and E. Malec, Binding energy for charged spherical bodies, Classical Quantum Gravity **7**, L199 (1990).
[23] K.-i. Nakao, M. Kimura, M. Patil, and P. S. Joshi, Ultrahigh energy collision with neither black hole nor naked singularity, Phys. Rev. D **87**, 104033 (2013).
[24] H.-O. Kreiss and O. E. Ortiz, *Introduction to Numerical Methods for Time Dependent Differential Equations*, 1st ed. (John Wiley & Sons, Hoboken, NJ, 2014).
[25] W. B. Bonnor, A model of a spheroidal body, Classical Quantum Gravity **15**, 351 (1998).
[26] R. Bartnik and J. Isenberg, in *The Einstein Equations and Large Scale Behavior of Gravitational Fields*, edited by P. T. Chruściel and H. Friedrich (Birhäuser Verlag, Basel, 2004), p. 1.